SCIENTIFIC REPORTS

OPEN

Universal optimal geometry of minimal phoretic pumps

Sébastien Michelin [1] & Eric Lauga [2]

Unlike pressure-driven flows, surface-mediated phoretic flows provide efficient means to drive fluid motion on very small scales. Colloidal particles covered with chemically-active patches with nonzero phoretic mobility (e.g. Janus particles) swim using self-generated gradients, and similar physics can be exploited to create phoretic pumps. Here we analyse in detail the design principles of phoretic pumps and show that for a minimal phoretic pump, consisting of 3 distinct chemical patches, the optimal arrangement of the patches maximizing the flow rate is universal and independent of chemistry.

The rapid development of microfluidics, which already has had a deep impact on both biology and chemistry[1–4], was enabled by key advances in continuum physics. Indeed, it is our understanding of the surface-dominated physics at the micron scale which has allowed the invention of a whole array of small-scale devices to precisely control flow and transport processes in microfluidic devices[5].

One of the standard issues in small devices is the difficulty of driving flows. In a straight channel, or pipe, the rate at which a Newtonian liquid flows from one side of the channel to the other scales as the fourth power of a relevant cross-sectional channel length scale times the applied external pressure gradient[6]. When length scales become tens of microns or less, the external pressures required to drive flows become prohibitively large and as a result the community has turned to surface-driven methods where a flow is induced locally[5,6].

In the biological world, surface flows are often created along tissues, or groups of cells, by the time-varying beating of short cilia[7] resulting in effective slip boundary conditions for the neighbouring flow[8,9]. Although artificial cilia have been realised in the lab, the dynamics and performance of biological ciliary arrays has proven difficult to reproduce experimentally[10–12].

Instead, a popular method to generate flows near surfaces in the lab consists in taking advantage of phoretic mechanisms where externally-applied physico-chemical gradients (such as charge, temperature, composition…) create local body forces on the fluid in thin layers near surfaces which, through the action of viscous stresses, entrain a bulk flow[13]. A famous example of such methods is electrophoresis wherein an electric field applied along a channel filled with an electrolyte drives a flow due to charge imbalance near the electrical double layer at the junction between the fluid and surfaces[5].

While externally-applied gradients are able to drive flows, gradients which are instead generated locally on the surface of colloidal particles can be used to generate locomotion[14–17]. Self-propulsion of such phoretic swimmers can result either from chemical gradients directly patterned on the particles themselves via coated catalysts[18] or from transport instabilities for chemically-homogenous particles[19–21], and have proven popular model systems in the field of active matter[22]. A canonical example of such catalytic reactions is the decomposition of hydrogene peroxide on platinuum-coated surfaces[14] or iron oxide catalysts[23], but many other chemical reactions have also been considered[24,25].

The physico-chemical principles used for phoretic swimmers can in principle also be exploited to induce flow transport in confined devices such as microchannels, and therefore to create pumps[26–29]. Yet, the existing literature has only so far provided limited insight on the fundamental design principles of such pumps, and we propose here a detailed analysis of the link between pump design and performance. In particular, with a view toward experimental realisation, an important practical question is that of minimal geometrical design. What type of surface chemistry would be simple to fabricate yet effective at creating transport?

In the case of swimmers, the minimal design is that of a Janus particle whose surface is covered by two distinct, homogeneous patches of which at least one is phoretically active. By symmetry, a Janus channel cannot be used to pump flows, and the simplest design has three patches. In this paper, we solve theoretically the P-patch problem. We demonstrate that in the minimal case of $P = 3$ patches, the optimal pump design, i.e. the geometrical

[1]LadHyX – Département de Mécanique, Ecole Polytechnique – CNRS, Institut Polytechnique de Paris, 91128, Palaiseau, France. [2]Department of Applied Mathematics and Theoretical Physics, University of Cambridge, Cambridge, CB3 0WA, United Kingdom. Correspondence and requests for materials should be addressed to S.M. (email: sebastien.michelin@ladhyx.polytechnique.fr) or E.L. (email: e.lauga@damtp.cam.ac.uk)

1
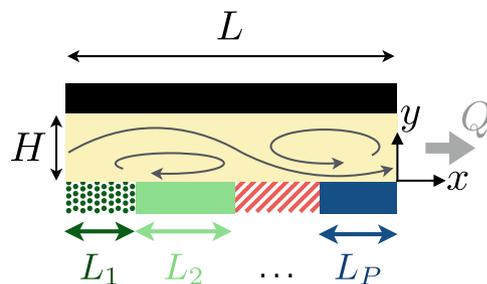
Figure 1. Periodic phoretic pump design: A straight, two-dimensional channel of width H is periodically coated with P chemically-active patches (per period L) of lengths $L_1, L_2, \ldots, L_P$ (transverse stripes in three dimensions). Diffusiophoresis leads to pumping with flow rate Q (schematic flow illustration).

arrangement of chemical patches leading to maximum phoretic flow rate, is universal and independent of chemistry, in stark contrast with Janus particles.

Results

Model and performance of a generic phoretic pump. We consider an infinite, straight two-dimensional channel of width H (Fig. 1). One of the channel walls, located at $y = 0$, is chemically-coated with a catalyst along a repeated pattern of period L. The catalyst allows a chemical reactant in the liquid to produce a new solute species of concentration $C(\mathbf{x})$. In the limit of large reactant concentration, we may assume that the solute release occurs at a fixed rate, or activity, $A(x)$,

$$D\frac{\partial C}{\partial y}\bigg|_{y=0} = -A(x),$$

(1)

where D is the molecular diffusivity of the solute. At sufficiently small length scales, both advective and unsteady transports are negligible and the dynamics of the solute concentration is purely diffusive, $D\nabla^2 C = 0$. For simplicity, we assume that the upper wall allows for free exchanges of solute with a chemical reservoir so that the product concentration along it is homogeneous, $C(y = H) = C_0$. These conditions uniquely determine the solute concentration within the channel as

$$C(x, y) = C_0 - \frac{L}{2\pi D}\sum_{n=-\infty}^{\infty}\frac{a_n}{n}\frac{\sinh\left[\frac{2n\pi(y-H)}{L}\right]}{\cosh\left[\frac{2n\pi H}{L}\right]}\exp\left(\frac{2i\pi n x}{L}\right),$$

(2)

with a_n the Fourier coefficients of $A(x)$ given by

$$a_n = \frac{1}{L}\int_0^L A(x)\exp\left(-\frac{2in\pi x}{L}\right).$$

(3)

Due to the differential affinity of the chemically-patterned wall with the reactant and product molecules, local surface gradients in solute concentration result in a net slip velocity outside a thin interaction layer providing an effective slip boundary condition for the flow velocity, $\mathbf{u}$, as[13]

$$(\mathbf{u}\cdot\mathbf{e}_x)|_{y=0} = M(x)\frac{\partial C}{\partial x}\bigg|_{y=0},$$

(4)

with $M(x)$ the local diffusiophoretic mobility along the wall. This mobility stems from the difference in affinity with the wall surface (or short-range interaction potential) between the solute and solvent molecules within a thin interaction layer[13]. This simple framework can be easily generalized to other phoretic mechanism, such as thermophoresis[13,30,31], or other geometries (e.g. axisymmetric channels or patterning of top and bottom walls).

Using the fundamental properties of Stokes' flow, the resulting flow rate induced by the phoretic pump through any cross-section $\mathcal{S}_x$ of the channel is given by[32]

$$Q = \int_{S_x}\mathbf{u}\cdot d\mathbf{S} = \frac{H}{2}\langle u_s(x)\rangle,$$

(5)

where $\langle\cdot\rangle$ is the average in x over a period $[0, L]$. Using Eqs (2), (4) and (5), the pumping rate Q is then obtained as

$$Q = -\frac{H}{D}\sum_{n=1}^{\infty}\tanh\left(\frac{2n\pi H}{L}\right)\text{Im}[a_n m_{-n}],$$

(6)

where m_n are the Fourier coefficients of the mobility $M(x)$.

As expected for phoretic problems in the diffusive limit, the pumping rate is a bilinear function of the activity, $A(x)$, and mobility, $M(x)$, and no pumping is possible if either is constant along the channel, nor if $M(x) = \lambda A(x) + \mu$ where λ and μ are two arbitrary constants. For a Janus-type channel patterning consisting of the repetition of two patches with properties (A_1, M_1) and (A_2, M_2), one can write

$$A(x) = \frac{A_2 M_1 - A_1 M_2}{M_1 - M_2} + \left(\frac{A_1 - A_2}{M_1 - M_2}\right)M(x).$$

(7)

Consequently, two-patch patterns do create a flow within the channel but are unable to pump, a result which was expected since such systems are left-right symmetric (i.e. $x \leftrightarrow -x$) with respect to the midpoint of any of the patches. This is of course a fundamental difference with phoretic propulsion of microparticles for which a minimal two-patched Janus patterning leads in general to locomotion[18].

Pumping rate of a P-patch channel. While realizing continuous variations of the chemical properties of the wall is experimentally difficult, a simple patterning consists of the periodic repetition of $P \geq 3$ patches: on each patch S_p of length L_p (with $\sum_{j=1}^{P} L_j = L$), both $A(x)$ and $M(x)$ are constant and take values A_p and M_p, i.e.

$$A(x) = \sum_{p=1}^{P} A_p \mathbf{1}_{S_p}(x), \quad M(x) = \sum_{p=1}^{P} M_p \mathbf{1}_{S_p}(x),$$

(8)

where $\mathbf{1}_{S_p}(x) = 1$ for $x \in S_p$ and $\mathbf{1}_{S_p}(x) = 0$ otherwise. The Fourier coefficients a_n and m_n can be obtained from Eq. (3), and the flow rate of the channel is computed from Eq. (6) as

$$Q/L = \sum_{n=1}^{\infty} \frac{h \tanh(2\pi n h)}{\pi^2 n^2} \sum_{p<q} \alpha_{pq} \sin(\pi n l_p)\sin(\pi n l_q)\sin\left(\pi n\left[l_p + 2\sum_{j=p+1}^{q-1} l_j + l_q\right]\right),$$

(9)

with $l_p = L_p/L$ the reduced length of S_p, $h = H/L$ the channel aspect ratio and $\alpha_{pq} = (M_p A_q - M_q A_p)/D$. This generic form expresses the pumping rate in the channel as the sum of pair interactions between patches, whose intensity depends on their lengths and the distance between their centers. Note that the flow rate Q depends on the $P(P-1)/2$ coefficients $\alpha_{pq} = -\alpha_{qp}$ rather than the $2P$ chemical characteristics (A_j, M_j) but α_{pq} may not be defined independently from each other. These coefficients also set the characteristic velocity scales generated in such pumps, which are similar to those for the flows generated by phoretic swimmers[18].

The optimal and minimal phoretic pump. Since channels with $P = 2$ can never pump, the minimal phoretic pump has $P = 3$ patches. In that case, using $\sum l_j = 1$, the pumping rate in Eq. (9) becomes (see Supplementary Material).

$$Q/L = (\alpha_{12} + \alpha_{23} + \alpha_{31}) \times \mathcal{G}(l_1, l_2, l_3, h),$$

with

$$\mathcal{G}(l_1, l_2, l_3, h) = \sum_{n=1}^{\infty} \frac{h(-1)^{n+1}\tanh(2\pi n h)}{\pi^2 n^2} \prod_{j=1}^{3} \sin(\pi n l_j),$$

(10)

and is the product of two functions: (i) $\mathcal{F}(A, M) = \alpha_{12} + \alpha_{23} + \alpha_{31}$ which depends exclusively on the chemical properties of the patches and (ii) $\mathcal{G}(l_1, l_2, l_3, h)$ which depends only on the geometry of both channel and patches. Note that the function $\mathcal{G}$, written here in a symmetric form with respect to $(l_i)_{1 \leq i \leq 3}$, is effectively a function of l_1, l_2 and h only (since $l_1 + l_2 + l_3 = 1$).

The chemical function $\mathcal{F}$ can be rewritten (using the convention $A_{j+3} = A_j$),

$$\mathcal{F}(A, M) = \sum_{j=1}^{3} (A_{j+1} - A_j)(M_j + M_{j+1}),$$

(11)

and can thus be interpreted as the sum of contributions of adjacent pairs of patches which each induces a net flow proportional to the mean mobility multiplied by the difference in activity. A similar result is at the heart of the self-propulsion of Janus microswimmers[18].

The explicit separation of the chemical and geometric dependences of the pumping rate in Eq. (10) confers a universality to the three-patch configuration: The variation of the flow rate with the geometric patterning of the channel is not affected by the values of the chemical activities or mobilities. In particular, this means that the optimal pump, found by maximising the function $\mathcal{G}$, is unique and identical for all chemistry.

The variation of $\mathcal{G}$ within the 2D parameter space $\mathcal{I}_3 = \{0 \leq l_1, l_2, l_3 \leq 1, \sum l_i = 1\}$ is shown in Fig. 2. For all aspect ratios h, $\mathcal{G}$ vanishes if any $l_j = 0$ (Janus limit), which are the boundary points on $\mathcal{I}_3$. The gradient of $\mathcal{G}$ with respect to (l_1, l_2) is given by

$$\left(\frac{\partial G}{\partial l_1}\right)_{l_2} = \sum_{n=1}^{\infty} \frac{h \tanh(2\pi n h)}{n\pi} \sin(n\pi l_2)\sin[n\pi(l_1 - l_3)],$$

(12)
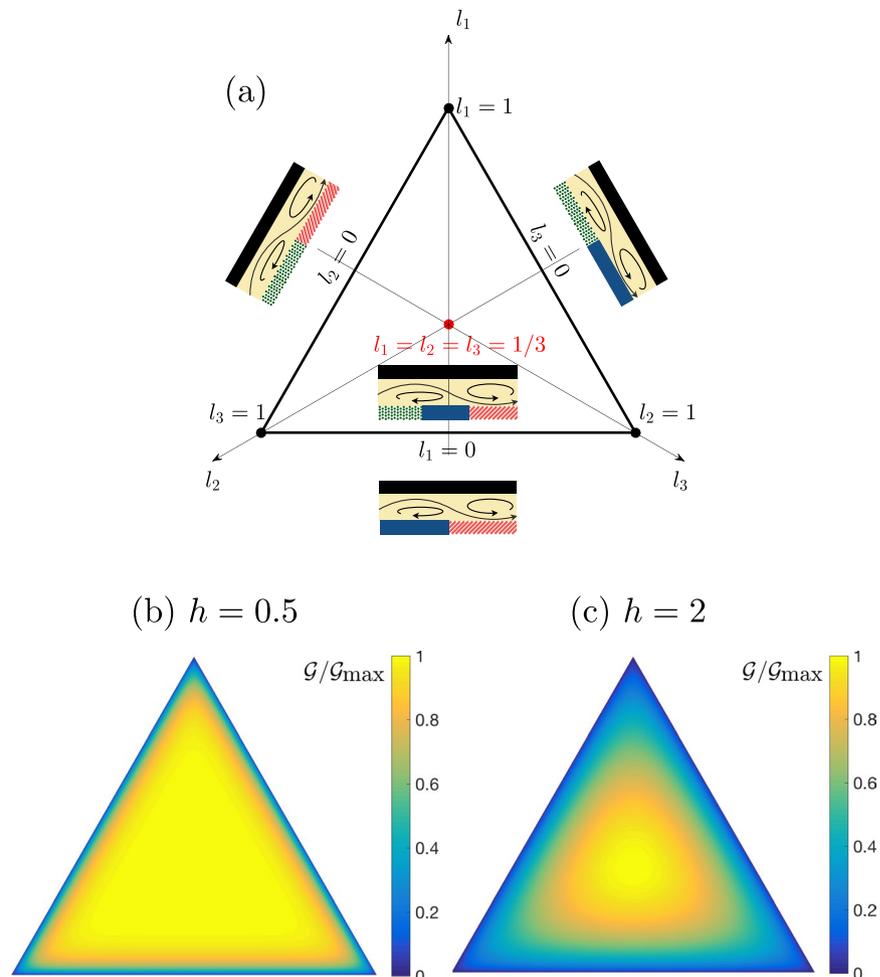
Figure 2. Influence of wall patterning on the performance of minimal 3-patch phoretic pumps. (**a**) Parametric representation of the geometric configuration (l_1, l_2, l_3) with $l_1 + l_2 + l_3 = 1$ (flow illustration is schematic). (**b,c**) Iso-values of the function $\mathcal{G}$ quantifying the contribution of the geometry of chemical patches to phoretic pumping for $h = 0.5$ (**b**) and $h = 2$ (**c**).

with $l_3 = 1 - l_1 - l_2$ and $(\partial G / \partial l_2)$ is obtained similarly; the only point within $\mathcal{I}_3$ where $|G|$ has a maximum is $l_1 = l_2 = l_3 = 1/3$, which confirms the results of Fig. 2. The optimal minimal (3-patch) pump is therefore unique and, independently of the chemistry, is the one where all patches have equal lengths.

The dependence of the pumping ability of the channel on its geometry can be further understood by examining the impact of the channel aspect ratio, $h = H/L$, on the optimal flow rate, $G_{\max}$ (Fig. 3). For large h, the flow rate varies linearly with h. In that case, the concentration distribution at the lower walls is independent of h at leading order, except for its mean value which does not contribute to pumping. The resulting phoretic slip forcing is therefore independent of h, and similarly to Couette (shear) flow, the net pumping is linear in h.

In the opposite limit, $h \ll 1$, the maximum flow rate scales quadratically with h (Fig. 3). In that case, the concentration profile is almost piecewise constant in x (i.e. away from the junctions between patches). Zooming in on the boundary between patches j and $j + 1$ for $x \approx x_j$, the leading-order concentration c can be rewritten as

$$C = C_0 + \frac{(A_j + A_{j+1})(H - y)}{2} + \frac{(A_j - A_{j+1})}{2} \widetilde{C}\left(\frac{x - x_j}{H}\right), \tag{13}$$

where $\widetilde{C}(s)$ is an odd function of s with $\widetilde{C}(\pm\infty) \pm 1$. Since $M(x)$ is piecewise constant near x_j, the resulting contribution of this junction to the pumping flow rate, $Q_{j,j+1}$, is obtained at leading-order for $h \ll 1$ as

$$Q_{j,j+1} = \frac{L(A_{j+1} - A_j)(M_j + M_{j+1})h^2}{4D}. \tag{14}$$

The total flow rate thus depends only on the junction between adjacent patches and is then obtained (for P patches) as
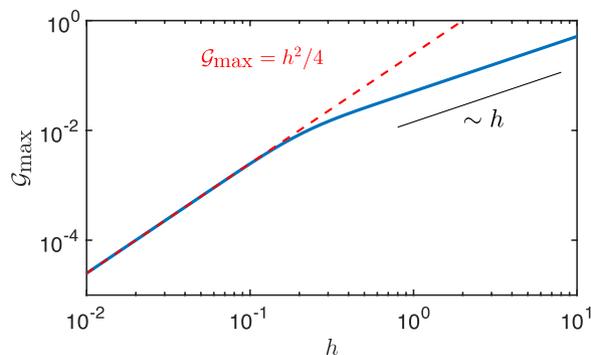
Figure 3. Influence of the pump aspect ratio on the performance of minimal 3-patch phoretic pumps. The dependence of the maximum pumping rate, G_{max}, on the channel aspect ratio $h = H/L$ is shown as well as the asymptotic prediction for $h \ll 1$ (dashed-red).

$$Q/L \sim \frac{h^2}{4D} \sum_{j=1}^{P} (A_{j+1} - A_j)(M_j + M_{j+1}) = \frac{h^2}{4} \sum_{j=1}^{P} \alpha_{j,j+1}. \tag{15}$$

Comparing with Eq. (10) for $P = 3$ shows that $\mathcal{G}_{max} = h^2/4$, in excellent agreement with the full solution (Fig. 3), and that $\mathcal{G} \approx \mathcal{G}_{max}$ when $h \ll 1$, as also observed on Fig. 2, demonstrating the robustness of the optimal design in that limit.

The universal nature of the optimal geometry for minimal ($P = 3$) phoretic pumps is intimately linked to the number of independent chemical properties setting the flow rate. For P patches, $2P$ different properties come into play, (A_i, M_i). Denoting by $\mathcal{A}$ and $\mathcal{M}$ a characteristic magnitude of activity and mobility, dimensional analysis imposes that $Q = \mathcal{A}\mathcal{M} \times \tilde{Q}$, and $\tilde{Q}$ depends on only $2(P-1)$ parameters. No net pumping is obtained if either $(A_i)_i$ or $(M_i)_i$ are all identical, or if both sets are linearly correlated, providing three additional constraints, such that the pumping rate effectively only depends on $2P - 5$ independent chemical parameters. For $P = 3$ patches, this confirms that a single chemical function controls the pumping rate, conferring its universality to the minimal pump.

Minimal phoretic swimmers vs. minimal phoretic pumps. While the minimal phoretic pump must include three different patches, minimal phoretic swimmers are able to break symmetries using only two. However, in contrast to the results obtained above and showing universality of the three-patch pump, the optimal minimal (Janus) swimmer is not universal but its geometry depends on the surface chemistry. This can be seen by evaluating the swimming velocity of an unit-radius axisymmetric Janus sphere coated with two different materials (A_1, M_1) on the portion $\mu \le z \le 1$ of its surface (front side) and (A_2, M_2) for $-1 \le z \le \mu$ (back). The result is

$$U = \frac{(A_2 - A_1)(1 - \mu^2)}{8}[M_1 + M_2 + (M_2 - M_1)V(\mu)],$$

with

$$V(\mu) = \mu^3 + 2 \sum_{n=2}^{\infty} \frac{(1 - \mu^2)L'_n}{n(n + 1)} \left(\frac{L'_{n-1}}{n} - \frac{L'_{n+1}}{n + 2} \right), \tag{16}$$

where $L'_n(\mu)$ is the derivative of the n-th Legendre polynomial[18]. The non-universality of Janus swimmers can then be demonstrated by highlighting a few examples. When $M_1 = M_2$, the Janus swimmer with maximum speed is hemispheric, and thus the optimal value is $\mu_{opt} = 0$. In contrast, when $M_1 = -M_2$, the hemispheric particle with $\mu = 0$ does not swim and the swimming speed is instead maximized for $\mu_{opt} \approx \pm 0.61$. The optimal Janus swimmer, i.e. the value of μ maximizing $|U|$, is therefore not universal and optimizing the patterning of the surface of the swimmer requires a detailed knowledge of its chemical properties, in contrast with minimal phoretic pumps which are always optimal for $l_i = 1/3$.

Optimal pumps beyond 3-patch patterns. The universality for pumps is lost for $P > 3$ as the pumping rate now depends on $2P - 5 > 1$ independent chemical parameters. In the case of $P = 4$ patches, the net flow rate, Eq. (9), becomes

$$Q/L = \sum_{j=1}^{4} \mathcal{F}_j(A, M)\mathcal{H}_j(l_1, l_2, l_3, l_4, h), \quad \text{with} \tag{17}$$

$$\mathcal{F}_1 = \alpha_{23} + \alpha_{34} + \alpha_{42}, \quad \mathcal{H}_1 = \sum_{n=1}^{\infty} \frac{h(-1)^{n+1} \tanh(2\pi nh)}{\pi^2 n^2} \cos(\pi nl_1) \prod_{k=2}^{4} \sin(\pi nl_k). \tag{18}$$
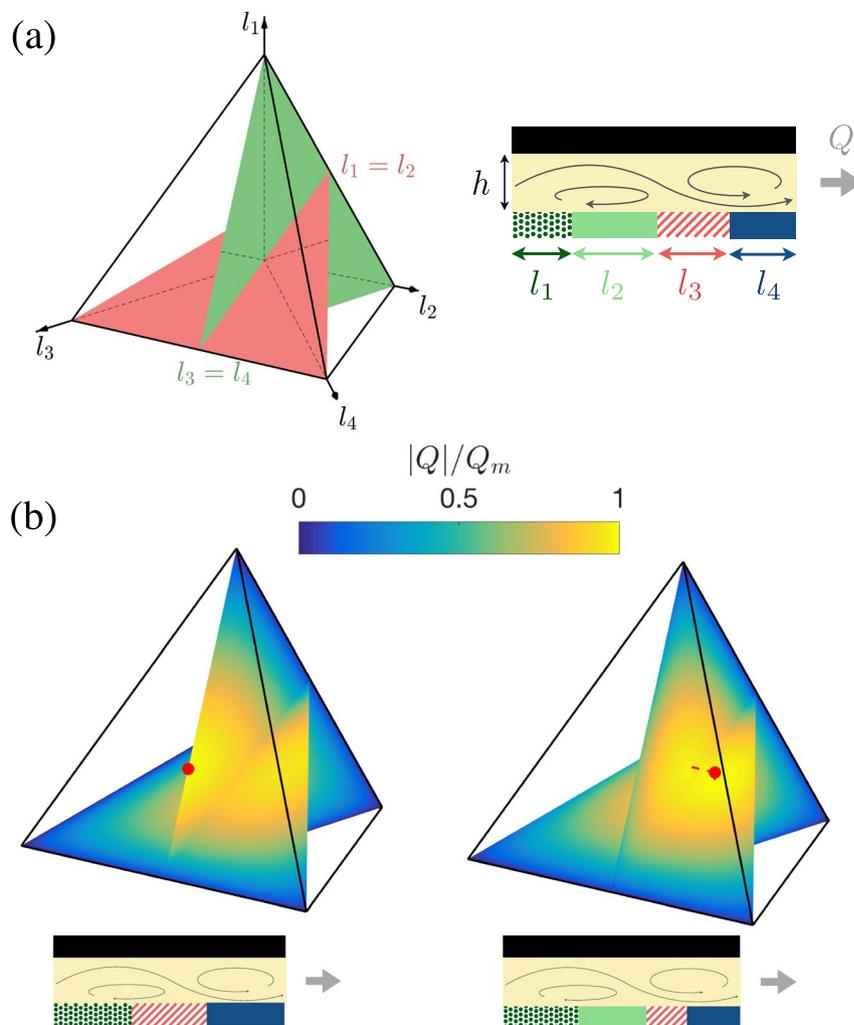
Figure 4. Optimal 4-patch phoretic pumps. (**a**) Parametric representation of the four-patch pump where each l_i is measured along a height of a regular tetrahedron. (**b**) The evolution with (l_i) of the flow rate visualized for $l_1 = l_2$ and $l_3 = l_4$ and two different fixed sets of chemical properties, one leading to an optimal degenerated pump (only three patches, left) and one with four different patch lengths (right). In each case, the parametric position of the optimal configuration is also shown (red point) together with the structure of the optimal pump. Degenerate pumps with only three patches correspond in this representation to the four faces of the tetrahedron, and as such the planar representation of Fig. 2 is simply the projection of the present figures on the particular subspace of interest.

with $\mathcal{F}_j$ and $\mathcal{H}_j$ obtained by circular permutation for $j \geq 2$ (see Supplementary Material). The $\mathcal{F}_j$ contribution is essentially a modulation of the 3-patch pump obtained for $l_j = 0$. The pumping rate nevertheless depends on only three independent parameters since these four contributions are not independent ($\mathcal{F}_1 + \mathcal{F}_3 = \mathcal{F}_2 + \mathcal{F}_4$). All possible geometries now span the three-dimensional parameter space $\mathcal{I}_4 = \{0 \leq l_1, l_2, l_3, l_4 \leq 1, \sum l_i = 1\}$. Depending on the surface chemistry, the optimal pumping rate is reached either (i) within $\mathcal{I}_4$ if $\mathcal{F}_1\mathcal{F}_3$ and $\mathcal{F}_2\mathcal{F}_4$ are both positive (non-trivial 4-patch pump) or (ii) on its boundary if either quantity is negative (degenerated 3-patch pump), in which case the universal optimal pump with three equal-length patches is recovered (see Supplementary Material). These two possibilities are illustrated on Fig. 4 where the dependence of the pumping efficiency on the geometry of patterning is represented over $\mathcal{I}_4$.

Discussion

In summary, this work proposes a generic mathematical framework to evaluate and optimize the phoretic pumping performance of a straight microchannel periodically-coated with active surfaces. Focusing on patterns which are well suited for experimental realization, namely a succession of materials with uniform chemical properties (patches), we show that the minimal pump features three different patches and is optimal for patches of equal lengths regardless of their chemical properties. Although we focused on diffusiophoresis, our results are also applicable to thermophoresis and electrophoresis (at least in the weak gradient limit when surface slip is proportional to the concentration gradient[13]) and could be extended to more complex geometries using numerical computations. For clarity and generality, we purposely focused here on the simplest chemical formulation of the problem, i.e. a prescribed fixed-flux of a single chemical component (reactant or product). Our framework could

nevertheless be extended to account for a more detailed description of the chemical reaction, for example by including several chemical components or multi-step reactions to describe the wall activity.

The most important result of our study is the universality of the optimal geometric design. This is a unique feature of the phoretic pumping problem that does not have an equivalent for phoretic swimmers. Furthermore, this universality is likely to be critical for experimental development since determining independently the chemical and phoretic properties of active materials is challenging experimentally. There is therefore no need for a trial-and-error experimental approach to phoretic pumps.

References

1. Whitesides, G. M. & Stroock, A. D. Flexible methods for microfluidics. *Phys. Today* **54**, 42–48 (2001).
2. Beebe, D., Mensing, G. & Walker, G. Physics and applications of microfluidics in biology. *Annu. Rev. Biomed. Eng.* **4**, 261–86 (2002).
3. Hansen, C. & Quake, S. R. Microfluidics in structural biology: Smaller, faster… better. *Curr. Opin. Struct. Biol.* **13**, 538–544 (2003).
4. Whitesides, G. M. The origins and the future of microfluidics. *Nat.* **442**, 368–373 (2006).
5. Squires, T. M. & Quake, S. R. Microfluidics: Fluid physics at the nanoliter scale. *Rev. Mod. Phys.* **77**, 977 (2005).
6. Stone, H. A., Stroock, A. D. & Ajdari, A. Engineering flows in small devices: Microfluidics toward a lab-on-a-chip. *Ann. Rev. Fluid Mech.* **36**, 381–411 (2004).
7. Sleigh, M. A., Blake, J. R. & Liron, N. The propulsion of mucus by cilia. *Am. Rev. Resp. Dis.* **137**, 726–741 (1988).
8. Blake, J. R. A spherical envelope approach to ciliary propulsion. *J. Fluid Mech.* **46**, 199–208 (1971).
9. Brennen, C. & Winnet, H. Fluid mechanics of propulsion by cilia and flagella. *Annu. Rev. Fluid Mech.* **9**, 339–398 (1977).
10. Fahrni, F., Prins, M. W. J. & van IJzendoorn, L. J. Micro-fluidic actuation using magnetic artificial cilia. *Lab Chip* **9**, 3413–3421 (2009).
11. Babataheri, A., Roper, M., Fermigier, M. & du Roure, O. Tethered fleximags as artificial cilia. *J. Fluid Mech.* **678**, 5–13 (2011).
12. Coq, N. *et al.* Collective beating of artificial microcilia. *Phys. Rev. Lett.* **107**, 014501 (2011).
13. Anderson, J. L. Colloid transport by interfacial forces. *Annu. Rev. Fluid Mech.* **21**, 61–99 (1989).
14. Howse, J. R. *et al.* Self-motile colloidal particles: From directed propulsion to random walk. *Phys. Rev. Lett.* **99**, 048102 (2007).
15. Ebbens, S. J. & Howse, J. R. Direct observation of the direction of motion for spherical catalytic swimmers. *Langmuir* **27**, 12293–12296 (2011).
16. Jülicher, F. & Prost, J. Generic theory of colloidal transport. *Eur. Phys. J. E* **29**, 27–36 (2009).
17. Moran, J. L. & Posner, J. D. Phoretic self-propulsion. *Annu. Rev. Fluid Mech.* **49**, 511–540 (2017).
18. Golestanian, R., Liverpool, T. B. & Ajdari, A. Designing phoretic micro- and nano-swimmers. *New J. Phys.* **9**, 126 (2007).
19. Thutupalli, S., Seemann, R. & Herminghaus, S. Swarming behavior of simple model squirmers. *New J. Phys.* **13**, 073021 (2011).
20. Michelin, S., Lauga, E. & Bartolo, D. Spontaneous autophoretic motion of isotropic particles. *Phys. Fluids* **25**, 061701 (2013).
21. Izri, Z., van der Linden, M. N., Michelin, S. & Dauchot, O. Self-propulsion of pure water droplets by spontaneous Marangoni stress driven motion. *Phys. Rev. Lett.* **113**, 248302 (2014).
22. Marchetti, M. C. *et al.* Hydrodynamics of soft active matter. *Rev. Mod. Phys.* **85**, 1143 (2013).
23. Palacci, J., Sacanna, S., Steinberg, A. P., Pine, D. J. & Chaikin, P. M. Living crystals of light-activated colloidal surfers. *Sci.* **339**, 936–940 (2013).
24. Duan, W. *et al.* Synthetic nano- and micromachines in analytical chemistry: sensing, migration, capture, delivery and separation. *Annu. Rev. Anal. Chem.* **8**, 311–333 (2015).
25. Yadav, V., Duan, W., Butler, P. J. & Sen, A. Anatomy of nanoscale propulsion. *Annu. Rev. Biophys.* **44**, 77–100 (2015).
26. Michelin, S., Montenegro-Johnson, T. D., Canio, G. D., Lobato-Dauzier, N. & Lauga, E. Geometric pumping in autophoretic channels. *Soft Matter* **11**, 5804–5811 (2015).
27. Shen, M. *et al.* Chemically driven fluid transport in long microchannels. *J. Chem. Phys.* **145**, 124119 (2016).
28. Yang, M. & Ripoll, M. Thermoosmotic microfluidics. *Soft Matter* **12**, 8564 (2016).
29. Tan, S., Yang, M. & Ripoll, M. Anisotropic thermophoresis. *Soft Matter* **13**, 7283 (2017).
30. Bickel, T., Majee, A. & Würger, A. Flow pattern in the vicinity of self-propelling hot janus particles. *Phys. Rev. E* **88**, 012301 (2013).
31. Baraban, L. *et al.* Fuel-free locomotion of janus motors: magnetically-induced thermophoresis. *ACS Nano* **7**, 1360–1367 (2013).
32. Michelin, S. & Lauga, E. A reciprocal theorem for boundary-driven channel flows. *Phys. Fluids* **27**, 111701 (2015).

Acknowledgements

Author Contributions
S.M. and E.L. designed research, performed the theoretical derivations, analysed data and wrote the paper.

Additional Information

Competing Interests: The authors declare no competing interests.

Publisher's note: Springer Nature remains neutral with regard to jurisdictional claims in published maps and institutional affiliations.